Supporting information

Periz et al. 10.1073/pnas.1220345110

SI Materials and Methods

DNA Design and Labeling. Oligonucleotides were designed using a positive-strand *segments 2, 6, or 11* as a template with amino-C6-dT modifications at the 5′ end. The Förster resonance energy transfer (FRET) efficiency E^* value of ∼0.35 was calculated using the Förster radius of the donor–acceptor pair (1) and the donor–acceptor separation (19–20 bp, ∼6.75–7.02 nm) on hybridization to the targeted transcript. The probes were relatively short (∼40 and ∼20 nt for the capture and FRET probes, respectively) to minimize formation of secondary structures, duplexes, or nonspecific binding, but still generate the required proximity. The probes targeted regions close to the 5′ end of single-stranded RNA (ssRNA) of *segments 2, 6, or 11* (ssRNA2, ssRNA6, and ssRNA11, respectively) while avoiding the conserved consensus sequence in the 5′ UTRs that may serve as assortment signals (2).

The sequence and modifications are in Table S1. Oligos T_2, T_6, T_{11}, $T_{6–11}$, T_{11}^{th}, C_2, C_6, and C_{10} were purchased as biotinylated forms (IBA), whereas C_{11} was biotinylated using sulfo-LC NHS biotin (Invitrogen). The other oligos were labeled at the 5′ end with either Cy3B or ATTO647N *N*-hydroxy-succinimidyl esters and purified using denaturing PAGE. Positive controls T_6-G_6-R_6, T_{11}-G_{11}-R_{11},$T_{(6-11)}$-G_6-R_{11} and G_{11}-Sp-R_{11}-R_{11}-$T(_{11}^{th})$ were prepared by mixing equimolar concentrations of oligos. For example T_{11}-G_{11}-R_{11} consisted of oligos T_{11}, G_{11}, and R_{11}. The annealing buffer consisted of 20 mM Tris, pH 8, 250 mM NaCl, and 1 mM EDTA. The oligo mixture was heated at 95 °C and left to cool slowly to 4 °C.

Synthetic RNA Control: T7 Synthetic Rhesus Monkey Rotavirus 11 Segment. cDNA copies of rhesus monkey rotavirus (RRV) 11 genomic segment were amplified from viral double-stranded RNA (dsRNA) in a sequence-independent manner using the method of full-length amplification of cDNAs (FLAC) (3, 4). Hairpin anchor primer C9 was ligated to viral dsRNA, followed by cDNA synthesis from gel-purified genome segments with RevertAid Premium reverse transcriptase (Fermentas) at a concentration of 10 U/μL and 55 °C for 1.5 h. PCR amplification was performed using FLAC 2 primer with KOD Hot Start DNA Polymerase (Novagen). PCR products were cloned and fully sequenced, and the T7 promoter and a suitable restriction site at the end were introduced to generate correct ends. Transcripts with a 5′-cap analog were generated from the digested T7 plasmid clones using a mMESSAGE mMACHINE T7 Ultra Kit (Ambion). Purified ssRNA were resuspended in nuclease-free water and stored at −80 °C.

Double-Layered Particle Purification. RRVs were kindly provided by H. Greenberg (Stanford, CA), and the double-layered particles (DLPs) were purified from rotavirus-infected cells as described (5). MA104 cells infected with RRV were harvested at 100% cytopathic effect; we used a multiplicity of infection (MOI) of 0.5–1 for growing stock viruses (propagation of the virus) and MOI of 3 for infection and purification of DLPs. Cells were disrupted by freezing and thawing twice, and EDTA (10 mM, pH 8) was added, followed by incubation for 1 h at 37 °C. After centrifugation, the pellet was resuspended in TNC buffer (10 mM Tris·HCl, pH 7.4, 140 mM NaCl, 10 mM $CaCl_2$) with 0.1% Nonidet P-40 and 50 mM EDTA, pH 8.0. Half volume of trichlorotrifluoethane was added to the lysate and mixed with vortex. The aqueous phase was separated by centrifugation, and DLPs were isolated by equilibrium ultracentrifugation at 100,000 × *g* in CsCl gradient for 18 h; the DLPs band was collected, diluted with TNC buffer, and pelleted by ultracentrifugation at 110,000 × *g* for 2 h.

Capture Assay of Transcripts in Solution. T7-derived positive-sense ssRNA11 (10 nM) was mixed with a hybridization buffer (100 mM Tris, pH 8.0, 9 mM $MgCl_2$, 150 mM NaCl, 0.5 U/μL RNase inhibitor), a FRET code that consisted of 10 nM each of G_{11} and R_{11} probes, and 10 nM capture probe C_{11}. The mixture was incubated for 1 h at 37 °C, and then aliquots were transferred to a total internal reflection fluorescence (TIRF)-alternating laser excitation (ALEX) microscope for analysis. The same hybridization method was performed for T7-derived positive sense ssRNA2, but using G_2 and R_2 FRET probes and capture probe C_2.

Transcription activity assays (5, 6) of DLPs were performed as above with the following modifications: DLPs (2 nM) were mixed with 20 nM of probes C6, G6, and R6. The sample was mixed in a transcription buffer of 100 mM Tris, pH 8.0, 4 mM ATP, 2 mM GTP, 2 mM CTP, 2 mM UTP, 9 mM $MgCl_2$, 150 mM NaCl, 0.5 mM S-adenosyl methionine (SAM), and 0.5 U/μL RNase inhibitor for 2 min at 37 °C, after which 2 mM EDTA was added to the reaction. Twenty-microliter aliquots were removed at time intervals of ∼1, 15, 30, 60, or 90 min, added to a slide for 2 min, and imaged using a PBS buffer with 1 mM 6-hydroxy-2,5,7,8-tetramethyl-chroman-2-carboxylic acid (TROLOX) (7) and an oxygen scavenger system (see sample preparation for details). The negative control consisted of an experiment in a transcription buffer but without nucleotides. The same hybridization method was implemented to capture ssRNA2 and ssRNA11 in solution but using specific FRET and capture probes for each transcript.

Capture Assay of Extruded Transcripts from DLPs. A suspension of DLPs in Tris, pH 8, was exchanged in PBS buffer using a Micro Bio-Spin 6 column (Bio-Rad). After that, 50 μL DLPs (2 nM) was mixed with the transcription buffer (50 mM phosphate buffer, pH 7.4, 1.4 mM KCl, 150 mM NaCl, 4 mM ATP, 2 mM GTP, 2 mM CTP, 2 mM UTP, 9 mM $MgCl_2$, 0.5 mM SAM, 0.5 U/μl RNase inhibitor) and incubated for 1 min at 37 °C. The transcription was stopped by fixing the DLPs with acidified glutaraldehyde (GT) vapor for 5 min at room temperature (8), followed by 5-min incubation with 150 mM Tris (pH 8.0) to quench the fixation reaction. The GT-containing buffer was then exchanged using a Micro Bio-Spin 6 column equilibrated in SSC buffer.

Hybridization to target ssRNAs templates was performed using a hybridization buffer, and conditions have been reported previously (9), but with several modifications. DLPs were mixed with 10 nM of C_6, G_{11}, and R_{11} and hybridization buffer consisting of 2× SSC, 9 mM citric acid (pH 6.0), 0.1% Tween-20, and 50 μg/mL heparin for 2 h at 50 °C. The hybridization buffer was then exchanged in SSC using a Micro Bio-Spin 6 column (Bio-Rad).

Capture was also performed to identify transcripts from *segment 6*; in this experiment, gentler hybridization conditions were introduced. Transcription was performed using the same buffer conditions optimized to capture segments in solution, but decreasing the concentration of nucleotides (1 mM ATP, 500 μM UTP, 500 μM GTP, 500 μM CTP). The reaction mixture was incubated for 2 min, and the reaction was then blocked using 4 mM EDTA. Probes G_6, R_6, C_{10}, and C_{11} (20 nM) were used, and the hybridization lasted for 1 h at 37 °C. Experiments were also performed to identify transcripts from *segment 2* using the

same conditions and probes G_2, R_2, C_6, and C_{11}. For the colocalization of *segments 6 and 11*, the experiment was performed as described above, but using capture probes C_6 and C_{11} and reporter probes G_6 and R_{11}. In colocalization experiments using RNA as a template, we synthesized the RNA using the same transcription conditions used in DLP capture experiments. The ssRNA was separated from the DLPs by 50-min centrifugation at 100,000 × *g* in an ultracentrifuge (rotor TLA 100.2, Optima TL; Beckman).

Capture of DLPs Bearing Extruded Transcripts Using Capture Antibodies. The experiment was performed as described previously (10) with some modifications. DLPs were allowed to transcribe for 2 min and fixed with 2% (wt/vol) paraformaldehyde for 5 min. DLPs were buffer-exchanged to SSC buffer using a micro Bio-Spin column (Bio-Rad) and interrogated using 20 nM of G_2 and R_2 FRET probes [which target (+)ssRNA2] for 2 h at 37 °C. DLPs were then buffer-exchanged in 10 mM Tris, pH 8, and 50 mM NaCl and incubated for 1 h with 66 nM sheep anti-VP6 (primary antibody ab35417; abCAM). Next, the DLPs were added for 5 min to a coverslip coated with biotinylated rabbit anti-sheep secondary antibody (ab6746; abCAM), prepared by incubating the coverslip with secondary antibody (26 nM in the same buffer conditions) for 30 min followed by a PBS wash. We used two negative controls to test nonspecific interactions of antibodies to DLPs: the first had the primary antibody substituted by rabbit γ-globulins (purified from nonimmunized rabbit serum, 011-000-002; Jackson ImmunoResearch), and the second was performed in the absence of biotinylated secondary antibody.

Sample Preparation. Biotinylated DNA constructs were bound to neutravidin-coated glass coverslides (11). These coverslides were prepared in the following way. Silicone gaskets (Grace Bio-Labs) were placed onto a neutravidin-treated coverslip, and a second coverslip used to seal the imaging chambers from oxygen. Imaging buffers were used in buffer PBS (pH 7.4). All imaging buffers contained an enzymatic oxygen scavenging system [10% (wt/vol) glucose, 1 mg/mL glucose oxidase, and 40 μg/mL catalase]. The imaging buffer contained 1 mM TROLOX.

ALEX Microscopy. Samples were imaged on a custom-built TIRF microscope, using ALEX (12). The red laser (635 nm, Cube model; Coherent) was directly modulated, and the green laser (532 nm, continuous wave, Samba model; Cobolt) was modulated with acousto-optical modulator (AA optics) with an alternation period of 100 ms. Because the imaging was performed using TIRF microscopy, which mainly detects signals within an evanescent field of ∼100 nm, the assay reflects mainly the fluorescence of surface-captured molecules or particles.

Laser beams were coupled into a single-mode optical fiber, and output from the fiber was collimated and directed into an inverted microscope IX71 Olympus through a 100× oil immersion Olympus objective, numerical aperture (NA) 1.4. The fluorescence emission is collected by the same objective and separated from the excitation path by a dichroic mirror (545/650 nm; Semrock) and additional filters (545 nm LP, Chroma; 632/25 nm notch filter; Semrock). Dual-color detection is achieved by splitting the emission light into red and green channels (630 DRLP; OMEGA) and projecting onto two regions of an EMCCD camera (iXon+; Andor). The intensities of the lasers were measured before the entry into the TIRF objective and were set to 1.5 (635 nm) and 0.75 mW (532 nm) for Cy3B and ATTO647N, respectively. Because the relative probe stoichiometry S signal depends on the relative brightness of the fluorophore, the laser powers were chosen to yield a value of $S \sim 0.5$ for a stoichiometry of 1:1 for the Cy3B–ATTO647N pair used in the FRET probes and the positive controls.

We note that 12.5% of the intensity detected in the green channel leaks into the red channel, which generates an apparent FRET baseline of $E^* = 0.11$ from a Cy3B-only signal. This FRET baseline is due to the imperfect color splitting and the natural spectral leakage of Cy3B into the red channel. The red channel intensity of ATTO647N when excited by the 532-nm laser is 3% of the intensity of Cy3B excited by the 532-nm laser (or ATTO647N excited by the 635-nm laser). Therefore, the apparent FRET is $E^* = 0.13$ when both donor and acceptor are present without actual FRET.

Data Analysis. Data analysis was performed as described (13). Briefly, the extraction of each single-molecule intensity trajectory was analyzed with custom software written in MATLAB (MathWorks) (13). The alignment of the green and red channels is performed with a peak-finding algorithm, and the emission intensities are filtered using ellipticity and nearest neighbor criteria ($\varepsilon < 0.7$, $NN > 5$ pixels) to eliminate colocalization artifacts due to the overlapping of two close point spread functions (PSFs). Three emission intensities are recorded from ALEX data: F_{DD} is the fluorescence intensity resulting from the donor emission on donor excitation; F_{DA} is the fluorescence intensity resulting from the donor emission on acceptor excitation; and F_{AA} (or $A_{ex}A_{em}$) is the fluorescence intensity resulting from the acceptor emission on acceptor excitation. These intensities are estimated by fitting a 2D Gaussian to each PSF. The apparent FRET efficiency, E^*, and relative fluorophore stoichiometry, S, were calculated by

$$E^* = \frac{F_{DA}}{F_{DD} + F_{DA}} \qquad S = \frac{F_{DD} + F_{DA}}{F_{DD} + F_{DA} + F_{AA}}.$$

Histograms display the combined data of movies recorded in identical conditions. Statistical analysis ANOVA (Tukey's test) and the t test were performed and plotted using GraphPad (GraphPad Software).

Correction of Nonuniform Illumination in the Field of View. In our experiments, the detected fluorescence intensity from a single molecule correlated significantly with the location of the molecule within the field of view. This correlation is mainly due to the nonuniform excitation field across the field of view, which has a profile that can be approximated by an elliptical 2D Gaussian. We have corrected for the nonuniform excitation (see $A_{ex}A_{em}$ intensity distributions in Figs. S1 and S4) as follows: for each molecule that emitted at a stable level (no photoblinking and no photobleaching), we calculated the mean intensity counts per frame $\overline{F}$ (e.g., in the acceptor channel) and localization position $(\bar{x}, \bar{y})$. A 2D Gaussian function of the form

$$f_F(x,y) = b + A \exp\left[-\frac{(x-\mu_x)^2}{2\sigma_x^2} - \frac{(y-\mu_y)^2}{2\sigma_y^2}\right] = b + A\phi(x,y)$$

was fitted to the set of experimental data points $\{\overline{F}(\bar{x},\bar{y})\}$, compiled from all single molecules detected in movies taken under identical conditions. The single-frame intensities F of a molecule found at $(\bar{x},\bar{y})$ were then corrected by

$$F^* = b + \frac{F-b}{\phi(\bar{x},\bar{y})},$$

corresponding to a mapping to a normalized intensity level $b + A$. In other words, F^* corresponds to the intensity one would observe if the position of the molecule were at (μ_x, μ_y), the maximum of the 2D Gaussian profile f_F. The corrected intensities are marked with an asterisk, i.e., $A_{ex}A_{em}{}^*$.

A single-molecule intensity time series $F = \{F_1, \ldots, F_{20}\}$ (20 × 100-ms ALEX frames) was determined to be stable if not more

than two consecutive frames showed intensity counts deviating from the median intensity more than two times the median absolute deviation (MAD)

$$\mathrm{MAD}(F) = \mathrm{Median}(\{|F_i - \mathrm{Median}(F)|\})$$

in both detection channels. MAD is a robust estimator for the SD s, and for normally distributed data, it can be shown that $\sigma \approx 1.48$ MAD.

Number of Colocalizations Observed vs. the Number Expected Due to Random Coincidence Even if the donor and acceptor particles localize independently, we still expect to detect colocalizations with our data analysis software Twotone due to the probability of probes coming closer than our colocalization search radius threshold of $R_{\mathrm{search}} = 250$ nm. A pair of donor and acceptor particles is considered as colocalized if the donor-acceptor distance is less than R_{search} and if no further donor or acceptor particles are present within a vicinity of $R_{\mathrm{exclude}} = 500$ nm from each of the particles under consideration. With the observed densities of donor and acceptor particles ρ_D and ρ_A in each field of view, the expected random colocalization density can be estimated as

$$\rho_{\mathrm{coloc}} = \pi R_{\mathrm{search}}^2 \rho_D \rho_A (1 - \pi R_{\mathrm{exclude}} \rho_D)(1 - \pi R_{\mathrm{exclude}} \rho_A).$$

This formula overestimates the number of detected random colocalizations because additional filters are in place to exclude particles with elliptical point spread functions (arising from closely spaced particles), as well as particles that fall below an intensity threshold. We determined ρ_D and ρ_A by counting the number of donor and acceptor particles in the homogenously illuminated part of the field of view and dividing by the area.

The number of observed colocalizations was tested against the number of estimated random colocalizations using a one-sided paired-sample Wilcoxon signed-rank in MATLAB (MathWorks). We used a paired test of the observed number and estimated number from the same movie, because both depend on the density of donor and acceptor signals. This test is preferable to a paired t test, as our test does not assume normally distributed data.

1. Holden SJ, et al. (2010) Defining the limits of single-molecule FRET resolution in TIRF microscopy. *Biophys J* 99(9):3102–3111.
2. McDonald SM, Patton JT (2011) Assortment and packaging of the segmented rotavirus genome. *Trends Microbiol* 19(3):136–144.
3. Boyce M, Celma CC, Roy P (2008) Development of reverse genetics systems for bluetongue virus: Recovery of infectious virus from synthetic RNA transcripts. *J Virol* 82(17):8339–8348.
4. Maan S, et al. (2007) Rapid cDNA synthesis and sequencing techniques for the genetic study of bluetongue and other dsRNA viruses. *J Virol Methods* 143(2):132–139.
5. Patton JT, Chizhikov V, Taraporewala Z, Chen D (2000) *Rotavirus, Methods and Protocols: Virus Replication*, eds Gray J, Desselberger U, (Humana, Totowa, NJ), pp 33–66.
6. Cohen J, Laporte J, Charpilienne A, Scherrer R (1979) Activation of rotavirus RNA polymerase by calcium chelation. *Arch Virol* 60(3-4):177–186.
7. Rasnik I, McKinney SA, Ha T (2006) Nonblinking and long-lasting single-molecule fluorescence imaging. *Nat Methods* 3(11):891–893.
8. Fadouloglou VE, Kokkinidis M, Glykos NM (2008) Determination of protein oligomerization state: Two approaches based on glutaraldehyde crosslinking. *Anal Biochem* 373(2):404–406.
9. Choi HM, et al. (2010) Programmable in situ amplification for multiplexed imaging of mRNA expression. *Nat Biotechnol* 28(11):1208–1212.
10. Chou YY, et al. (2012) One influenza virus particle packages eight unique viral RNAs as shown by FISH analysis. *Proc Natl Acad Sci USA* 109(23):9101–9106.
11. Roy R, Hohng S, Ha T (2008) A practical guide to single-molecule FRET. *Nature Methods* 5(6):507–516.
12. Margeat E, et al. (2006) Direct observation of abortive initiation and promoter escape within single immobilized transcription complexes. *Biophys J* 90(4):1419–1431.
13. Uphoff S, et al. (2010) Monitoring multiple distances within a single molecule using switchable FRET. *Nat Methods* 7(10):831–836.

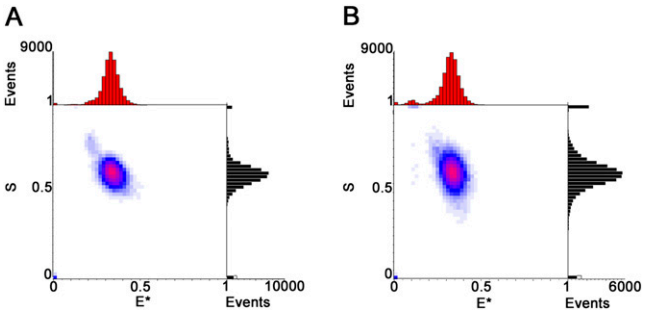

Fig. S1. The copy number of specific transcripts during their extrusion from transcriptionally active DLPs using a novel single-molecule fluorescence assay for transcript capture and identification (CID) assays for ssRNA11 and ssRNA6 transcripts produced by rotavirus DLPs. ssRNAs were incubated with capture and FRET probes, captured on the surface, and detected using ALEX-TIRF. (*A*) (+)ssRNA11 detected using G_{11} and R_{11} FRET probes and capture probe C_{11}. Combined *E*/S* histogram data of 2,553 detected particles with an *E*/S* signature of 0.35/0.55, well matching the code of 0.35/0.5. (*B*) (+)ssRNA6 detected using G_6 and R_6 FRET probes and capture probe C_6. Combined *E*/S* histogram data of 2,696 detected particles with an *E*/S* signature of 0.35/0.6, well matching the code of 0.35/0.5.

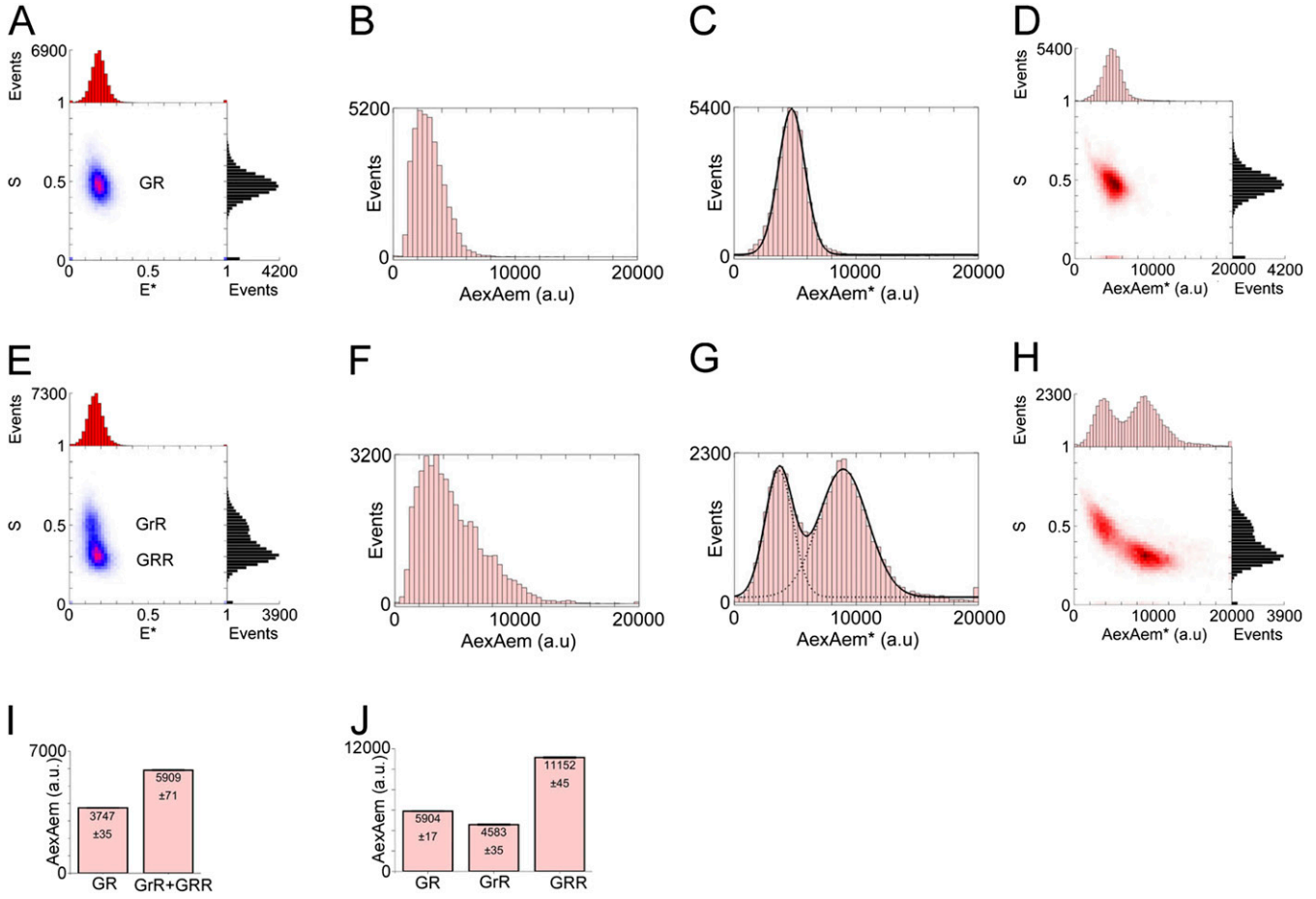

Fig. S2. Standards analyzed using *E*/S* histograms and fluorescence intensities. (*A*) *E*/S* histogram of dsDNA construct G_6-R_6-$T_{(6\text{-}11)}$ (a GR standard, meaning that the construct has one green labeled hybridized probe "G" and one red labeled hybridized probe "R"), compiled from 1,959 particles. The long fluorophore separation (40 bp) leads to negligible FRET. The population at $S \sim 0.5$ has the signal expected from constructs carrying one red and one green fluorophore. (*B*) Histogram of $A_{ex}A_{em}$ intensities for the GR standard (mean ± SEM: 3,747 ± 35 a.u.). (*C*) As in *B*, but corrected for nonuniform illumination (corrected emission intensities, $A_{ex}A_{em}$*). The fitted Gaussian function was centered at 5,904 ± 17 a.u. (*D*) $S/A_{ex}A_{em}$* histogram of the GR constructs shows that the well-defined population of $S \sim 0.5$ corresponds to a well-defined population of $A_{ex}A_{em}$* intensity centered at 5,909 a.u. (*E*) *E*/S* histogram of dsDNA construct G_{11}-Sp-R_{11}-R_{11}-$T_{(11^{th})}$ (a GRR standard, meaning that the construct has one green labeled hybridized probe "G" and two red labeled hybridized probes "R"). The long fluorophore separation (47 bp) leads to negligible FRET. The histogram (2,247 particles) shows a major population at $S \sim 0.3$ and a minor population at $S \sim 0.5$, consistent with a main population of fully hybridized constructs (GRR) and a minor population with a single R probe (GrR, meaning that the construct has one green labeled hybridized probe "G" but only one red labeled hybridized probe "R" out of the two sites available to red labeled probes; GrR is photophysically equivalent to the GR standard). (*F*) Distributions of $A_{ex}A_{em}$ intensities (5,909 ± 71 a.u.) from GRR samples, with 26% of GRR particles showing intensities >7,500 a.u. (cf. 1.5% of GR in *B*). (*G*) Distributions of $A_{ex}A_{em}$* intensities, revealing two well-resolved populations centered at 4,583 ± 35 and 11,152 ± 45 a.u., both fit to Gaussian functions. The lower intensity for GRR compared with the GR standard may indicate fluorophore interactions with the nonhybridized portion of DNA. (*H*) Two distinct $A_{ex}A_{em}$* populations can also be visualized on the S*/$A_{ex}A_{em}$* histogram. (*I* and *J*) Mean values and Gaussian fit results with error estimates.

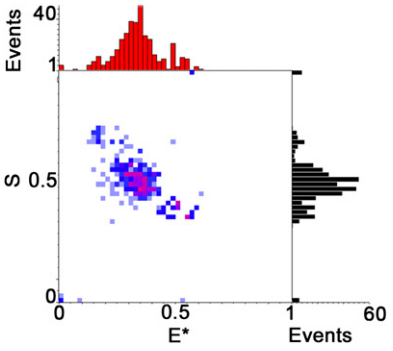

Fig. S3. Transcriptionally active DLPs carry a single extruded transcript for *segment 6*. CID of actively transcribing DLPs (allowed to transcribe for 2 min) were interrogated using capture probe C_{11} [which targets extruded (+)ssRNA11] and FRET probes G_6 and R_6 [which target extruded (+)ssRNA6]. The hybridization conditions are as described for capturing ssRNA6 using two capture probes. Combined *E*/S* histogram data of 38 detected particles show a main population centered at 0.35/0.5, which is the expected *E*/S* code for this transcript.

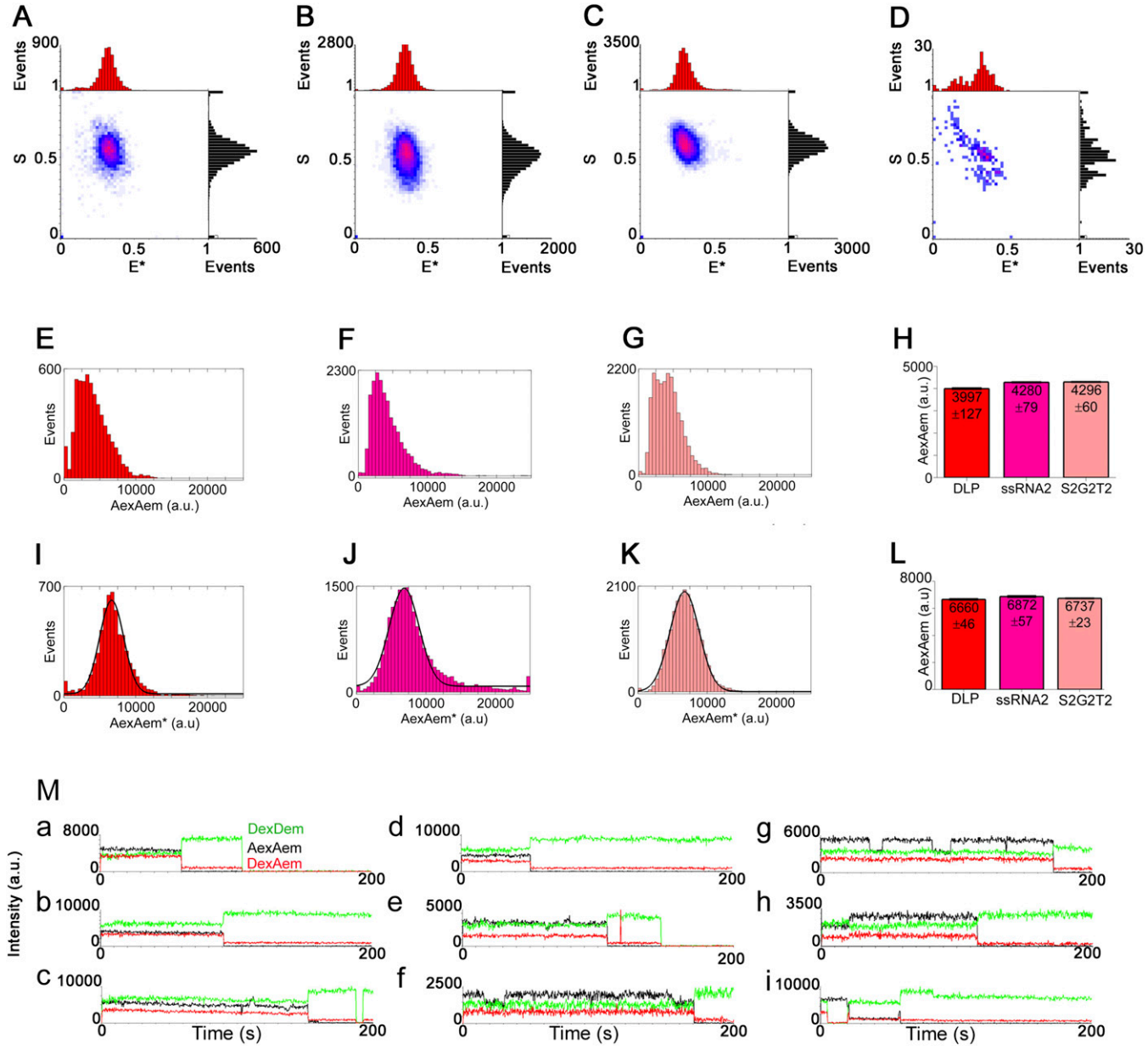

Fig. S4. Transcriptionally active DLPs carry a single extruded transcript for *segment 2*. (*A*) Actively transcribing DLPs (allowed to transcribe for 2 min) interrogated using capture probes C_6 and C_{11} and FRET probes G_2 and R_2 [which target extruded (+)ssRNA2]. The *E*/S* histogram (292 particles) shows a population of 0.35/0.5, matching the positive control (*B* and *C*). (*B*) Positive control. *E*/S* histogram (998 particles) of synthetic ssRNA2 hybridized with G_2 and R_2 and captured on the surface with capture probe C_2. (*C*) Positive control. *E*/S* histogram (1,079 particles) of G_2-R_2-T_2 dsDNA construct that consists of one G_2 and one R_2 probe hybridized to biotinylated T_2 ssDNA. (*D*) Negative control. *E*/S* histogram (11 particles) experiment performed with DLPs and FRET probes but without capture probes shows very few particles attached to the surface. (*E–G*) Distributions of average $A_{ex}A_{em}$ intensities from the sample in *A* (red), *B* (dark pink, positive control), and *C* (light pink, positive control). (*H*) Comparison of mean $A_{ex}A_{em}$ from ssRNA2 extruded in DLPs shown in *E* (red), captured ssRNA2 (*F*, dark pink, positive control), and dsDNA control (*G*, light pink). (*I–K*) Corrected $A_{ex}A_{em}$* intensity distributions from *A–C*, respectively, along with single Gaussian fits. (*L*) Mean $A_{ex}A_{em}$* intensity from the Gaussian fits for DLPs (*E*), ssRNA2 (*F*), and dsDNA control (*G*). (*M*) Photobleaching examples of DLPs captured with extruded ssRNA2 (39 particles). CID was performed as in *A* but taking longer movies (2,000 frames, 100-ms frames in *A–E* and *I* and 50-ms frames in *F–H*). Approximately 90% of the particles showed a single photobleaching step in the acceptor channel, whereas 10% displayed complex photophysics (see *I*).

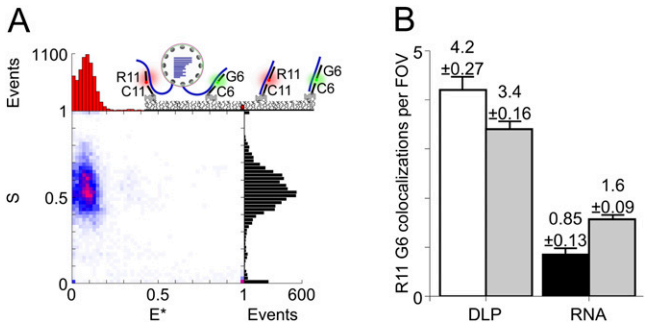

Fig. S5. Colocalization of (+)ssRNA6 and (+)ssRNA11 on DLPs. (*A*) CID of actively transcribing DLPs (allowed to transcribe for 2 min) interrogated using probes C_6 and G_6 [which target extruded (+)ssRNA6] and probes C_{11} and R_{11} [which target extruded (+)ssRNA11]. The *E*/S* histogram ($n = 357$, 80 movies) showed the expected *E*/S* value of ∼0.1/0.5, matching that of the positive control (*B*). (*B*) Comparison of the mean number of observed colocalizations per 25 × 25-μm field of view, with the mean estimated number of random colocalizations (gray columns; all error bars: SEM). For each field of view, the expected number of random colocalizations was calculated using the number of R_{11} and G_6 particles in each field of view. For the DLP experiment in *A* (white column), use of the one-sided paired-sample Wilcoxon signed-rank test showed that significantly more colocalizations were observed than expected by random colocalization ($P = 0.0004$; on average, 90 R_{11} and 183 G_6 particles). For the RNA experiment, fewer colocalizations were observed (black column; 34 colocalizations in 40 movies) than expected due to random colocalization; therefore, $P = 1$ (on average, 66 R_{11} and 98 G_6 particles per field of view). A control experiment using the same hybridization conditions as for the DLP sample but without the addition of nucleotides led to the capture of only two colocalized particles (20 movies) and no significantly higher colocalization than expected by chance ($P > 0.05$; on average, 1.8 R_{11} and 5.6 G_6 signals per field of view).

Table S1. Oligonucleotide DNA used in this study

Oligo	Segment sequence	Oligo sequence	Modification
G_6	(+17/+36)B	5′-ACAGGACATCCATGTTGAAG-3′	Cy3B 5′end
R_6	(+37/+56)B	5′-AAGAGTTTTTGACAAGGAGT-3′	ATTO647N 5′end
T_6	(+14/+56)T	5′-AGTCTTCAACATGGATGTCCTGTACTCCTTGTCAAAAA CTCTT-3′	Biotin 5′end
C_6	(+56/+95)B	5′-GTATAATGTGCCTTCGTCAATTTTGACTCTAGCATCTT TA-3′	Biotin 5′end
C_{10}	(+21/+40)B	5′-TTTCCGCACGCGCTCTCTCG-3′	Biotin 5′ end
G_{11}	(+16/+35)B	5′-ATACTGAGAGACATCACTGT-3′	Cy3B 5′end
R_{11}	(+36/+54)B	5′-TGGAAGACTTGTCACGTCA-3′	ATTO647N 5′end
T_{11}	(+15+54)T	5′-TACAGTGATGTCTCTCAGTATTGACGTGACAAGTCTTC CA-3′	Biotin 5′end
C_{11}	(+55+94)B	5′-TGAAGATGATTCATGTTTATAAATGCTGGAGGAAATA GA-3′	Biotin 5′end
$T_{(6\text{-}11)}$	Hybrid template	5′-AGTCTTCAACATGGATGTCCTGTTCC AAGTTAAGTGATCTA ATTCAACTGA CGTGACAAGTCTTCCA-3′	Biotin 5′end
$T_{(11^{th})}$	Hybrid template	5′-ACAGTGATGTCTCTCAGTATTCCAAGTTAAGTGATCTAATTCAA CTGACGTGACAAGTCTTCCATGACGTGACAAGTCTTCCA-3′	Biotin 5′end
Sp	(spacer sequence)	5′GTTGAATTAGAAGATCACTTAACTTGGA3′	
G_2	(+41+60)B	5′-TTTAAATTCGTCTCACGACG-3′	Cy3B 5′end
R_2	(+61+79)B	5′-TTGCATTCGATCATCTTGT-3′	ATTO647N 5′end
T_2	(+41+79)T	5′-CGTCGTGAGACGAATTTAAAACAAGATGATCGAATGCAA-3′	Biotin 5′end
C_2	(+21+40)B	5′-CGCTCCACGCTTTCTGTACG-3′	Biotin 5′end

Oligos are described with a capital letter that indicates the type of probe and labeling used followed by a subscript indicating the segment. The (+) ssRNA sequences are named as top strand (T) and numbered from the 5′ end (+1). Oligo sequences are designed using the (+)ssRNA as a template; B denotes bottom strand complementary to a sequence in the T strand. G is a green FRET probe labeled with Cy3B; R is a red FRET probe labeled with ATTO647N corresponding to the segment used as a template; C is a capture probe labeled with biotin. Sp is a spacer sequence based partially on a ssRNA6 genomic sequence, and is part of the long dsDNA control which consisted of one G_{11} and two R_{11} probes hybridized to complementary sequence $T(_{11}{}^{th})$. Sp minimizes the flexibility and nonspecific hybridization of probes in the G_{11}-Sp-R_{11}-R_{11}-$T(_{11}{}^{th})$ construct.